Transmission enhancement through square coaxial aperture arrays in metallic film: when leaky modes filter infrared light for multispectral imaging

Benjamin Vial,[1,2,*] Mireille Commandré,[1] Guillaume Demésy,[1] André Nicolet,[1] Frédéric Zolla,[1] Frédéric Bedu,[3] Hervé Dallaporta,[3] Stéphane Tisserand,[2] and Laurent Roux[2]

[1]*Aix Marseille Université, CNRS, Centrale Marseille, Institut Fresnel, UMR 7249, 13013 Marseille, France*

[2]*Silios Technologies, ZI Peynier-Rousset, rue Gaston Imbert Prolongée, 13790 Peynier, France*

[3]*Aix Marseille Université, CNRS, CiNaM, UMR 7325, Campus de Luminy, Case 913, 13288 Marseille Cedex 9, France*

**Corresponding author: benjamin.vial@fresnel.fr*

Received March 17, 2014; revised July 4, 2014; accepted July 4, 2014;
posted July 9, 2014 (Doc. ID 208244); published August 6, 2014

The diffractive behavior of arrays of square coaxial apertures in a gold layer is studied. These structures exhibit a resonant transmission enhancement that is used to design tunable bandpass filters for multispectral imaging in the 7–13 μm wavelength range. A modal analysis is used for this design and the study of their spectral features. Thus we show that the resonance peak is due to the excitation of leaky modes of the open photonic structure. Fourier transform infrared (FTIR) spectrophotometry transmission measurements of samples deposited on Si substrate show good agreement with numerical results and demonstrate angular tolerance of up to 30 degrees of the fabricated filters.

OCIS codes: (220.0220) Optical design and fabrication; (050.1755) Computational electromagnetic methods; (050.5745) Resonance domain; (050.6624) Subwavelength structures; (110.4234) Multispectral and hyperspectral imaging; (220.4241) Nanostructure fabrication.

http://dx.doi.org/10.1364/OL.39.004723

Nanostructuration of metallic surfaces at subwavelength scale can lead to spectacular resonant effects [1]. In particular, annular aperture arrays (AAAs) have recently drawn considerable attention because of their potential application as highly integrated photonic components since the work of Baida and co-workers [2–7] demonstrating enhanced transmission properties in such structures. AAAs have also been designed and studied experimentally at mid-IR wavelengths by Fan *et al.* [8,9]. Another key property of AAAs is the angular tolerance of the enhanced transmission as demonstrated theoretically in [5,10]. Experimental verification of angular independent response has been reported in AAAs and various metamaterial structures for transmission and reflection filters [8,11–13].

In this Letter, we consider arrays of square coaxial apertures in a gold film deposited on a silicon substrate that are designed to produce bandpass transmission filters for multispectral imaging applications in the far infrared region. The spectral range 7–13 μm (infrared band 3) corresponds to a transparency window of the atmosphere and therefore adding multispectral filtering capabilities to infrared sensors in this range is of crucial importance in applications such as detection and discrimination of chemical compounds or vegetation recognition. Multispectral filters in this wavelength range must have a large width and maximum transmission level to obtain sufficiently high intensity on the detector. Moreover multispectral imaging applications require angular tolerance of the filter central wavelength. Finally in this study only transverse dimensions of the arrays are modified in order to fabricate all the filters on the same substrate in a single lithography step leading to a low-cost process.

Besides the calculation of transmission spectra, our approach to study the resonant phenomena in such metamaterials is to compute the eigenmodes and eigenfrequencies of such open electromagnetic systems. This modal approach leads to significant insights into the properties of metamaterials [14,15] and eases the conception of diverse optical devices [16,17] because it provides a simple picture of the resonant processes at stake. We used this modal approach to design the tunable filters of this Letter.

The square coaxial apertures have interior and exterior width denoted w_1 and w_2, respectively, and are arranged in a square array of period d [see the inset in Fig. 2(a)]. The thickness of the metallic film is $h = 90$ nm, which is higher than the skin depth of gold in the investigated wavelength range so that the unstructured layer is optically opaque.

First, we investigate transmission properties of AAAs by numerical simulations. A finite element method (FEM) formulation already described in Refs. [18,19] is used to solve the so-called *diffraction problem*. The array is illuminated from the air superstrate by a plane wave of radial angle θ_0, azimuthal angle φ_0, and polarization angle ψ_0. The permittivity of gold is described by a Drude–Lorentz model [20] and the refractive index of silicon is taken from tabulated data [21]. All materials are assumed to be nonmagnetic ($\mu_r = 1$). We model a single period with Bloch conditions applied in x and y directions of periodicity such that the electric field $\boldsymbol{E}$ is quasi-periodic: $\boldsymbol{E}(x + d_x, y + d_y, z) = \boldsymbol{E}(x, y, z)e^{i(\alpha d_x + \beta d_y)}$, where $\alpha = -k_0 \sin\theta_0 \cos\varphi_0$ and $\beta = -k_0 \sin\theta_0 \sin\varphi_0$ are the tangential components along x and y of the incident wavevector $\boldsymbol{k}_0$. Perfectly matched layers (PMLs) are used in the z direction normal to the grating in order to damp propagating waves [22,23].

Because of the resonant nature of the transmission spectra, we performed a modal analysis [24] of these structures. We use a FEM formulation to solve the

spectral problem, i.e., to find leaky modes (also known as quasi-modes, quasi-normal modes, or resonant states) associated with complex eigenfrequencies $\omega_n = \omega'_n + i\omega''_n$ of the open nanoresonators [13], the real part corresponding to the resonant frequency and the imaginary part to the linewidth of the resonance. The quasi-modes are an intrinsic property of the system and are very useful to characterize the resonant process at stake. This approach allows us to compute quickly the features of the resonance and their evolution when the geometric parameters of the AAA are changed. The FEM formulation is analog to the diffraction problem except that there are no sources. Bloch conditions are applied with fixed real quasi-periodicity coefficients α and β along x and y, and PMLs are used in the direction orthogonal to the array. As a first approximation, the materials are assumed to be nondispersive, which makes the spectral problem linear. To take into account dispersion, the eigenvalue problem is solved iteratively with updated values of permittivity. This procedure converges rapidly due to the slow variations of the permittivity of the considered materials in the far infrared range.

For a given grating, three transverse geometrical parameters are necessary to characterize the pattern of coaxial apertures: w_1, w_2, and d. We solved the spectral problem with $\alpha = \beta = 0$ for homothetic structures with $d = 2.4$ μm, $f_2 = w_2/d = 0.55$, and various periods d, such that all AAAs have the same opening area ratio $\rho = (w_2^2 - w_1^2)/d^2 = f_2^2(1 - f_1^2) = 10.9\%$. This homothetic scaling allows us to cover the entire spectral range 7–13 μm. Because of the symmetry of the problem, we find two degenerated eigenmodes corresponding to TE and TM polarization associated with the same eigenfrequency ω_1. We have represented in Fig. 1(a) the evolution of the resonant wavelength $\lambda^r = 2\pi c/\omega'$ as a function of d for the TM mode (red crosses). The evolution is linear and fits well with the formula $\lambda^r = 3.91d + 0.52$ (thin black line). We also extracted the resonant wavelength corresponding to the maximum values of calculated transmission spectra, and reported it as a function of d in Fig. 1 (top) (thick blue line). The agreement with the results of the spectral problem is excellent. In addition, the imaginary part of the eigenfrequency $\omega_{1''}$ is equal to $2\Delta\omega$, where $\Delta\omega$ is the spectral width of the resonance. We can thus obtain the spectral width in terms of wavelength from the expression $\Delta\lambda = -4\pi c\omega''/\omega'^2$ and plot it as a function of d on Fig. 1(b), red crosses). The evolution is also linear (fitted by $\Delta\lambda = 1.12d - 0.10$, thin black line) and matches the values of the full width at half the maximum obtained from the calculated transmission spectra (thick blue line). Field maps corresponding to the electric and magnetic field intensity of this resonant mode for $d = 2.4$ μm are plotted on Figs. 1(c) and 1(d), respectively. The electromagnetic field is concentrated in the annular apertures and further study of the field maps confirms that this mode behaves as a TE_{11}-like mode [3]. These results demonstrate that the resonant transmission enhancement is mainly due to the excitation of a single leaky mode supported by the AAA.

The modal analysis allows us to design four filters with a given central wavelength $\lambda^r = 8$, 9.7, 10.3, and 12 μm thanks to the linear fit. We thus obtain the geometric parameters of the filters denoted M1, M2, M3, and M4,

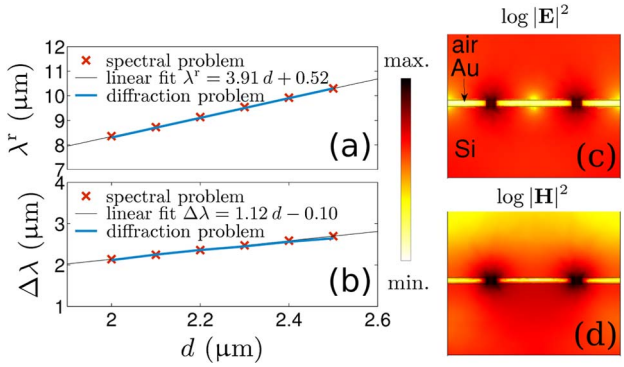

Fig. 1. Spectral parameters of the resonance as a function of the period d obtained from calculated transmission spectra (blue line) and extracted from the degenerated eigenfrequencies (red crosses). (a) Resonant wavelength and (b) spectral width. (c) Electric and (d) magnetic field maps of the leaky mode in the *Oyz* plane for $d = 2.4$ μm.

respectively: $d = 1920$, 2250, 2600, 2930 nm, $w_1 = 850$, 990, 1140, and 1290 nm and $w_2 = 1060$, 1240, 1430, and 1610 nm. These structures are homothetic such that $f_1 \simeq 0.8$ and $f_2 \simeq 0.55$. Calculated transmission spectra in the specular diffraction order $T_{0,0}$ under normal incidence in TM polarization are reported in Fig. 2(a). Note that the order (n, m) is evanescent for $\lambda > d\sqrt{\varepsilon^-/(n^2 + m^2)}$ but for all filters, the transmission associated with propagative orders other than $(0, 0)$ is very weak (<1.5%) on the studied spectral range. The transmissions show a resonant peak whose central wavelength can be redshifted by increasing solely the lateral dimensions of the AAA. The spectral width varies from 2 to 3 μm as lateral dimensions increase. The maximum transmission value remains unchanged around 0.58 and quality factor $Q = \omega^r/\Delta\omega \simeq 3.8$ is nearly constant because all structures have the same opening area ratio. The Fano resonances at shorter wavelengths ($\sim d\sqrt{\varepsilon^-/2}$) are due to the coupling of incident

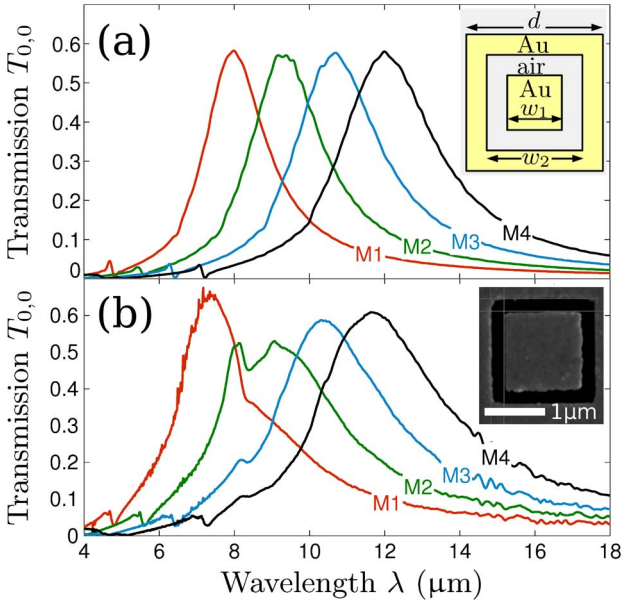

Fig. 2. Transmission spectra at normal incidence in the specular order $T_{0,0}$ as a function of incident wavelength λ for the different filters. (a) FEM simulations and (b) FTIR measurements.

wave with the Wood's anomaly associated with transmitted orders $(\pm 1, \pm 1)$ and the surface plasmon of Au–Si interface.

Samples with the aforementioned parameters have been fabricated on the same double size polished (100) pure intrinsic silicon substrate. The nanostructuration was performed by electronic lithography using a liftoff process with a negative tone resist to obtain a relatively large nanostructured area of 3 mm × 3 mm for each of the four samples to allow the measurements of FTIR spectra. Transmission spectra of the samples have been recorded with a Thermo Fisher-Nicolet 6700 Fourier transform infraRed (FTIR) spectrophotometer. Measurements were performed with a focused polarized light beam with ±16° divergence and a spot diameter of 1.3 mm. A rotating deck allows us to tilt the sample in order to record transmission spectrum for incident angles between 0° and 90°. All the spectra are normalized with a background recorded with the substrate alone. The measured spectra at normal incidence and in TM polarization are reported on Fig. 2(b) and show good agreement with the simulated ones, even if the experimental resonances are slightly blueshifted and broader because of variations on the fabricated aperture widths. The transmission levels at resonance are of the order of 0.6 which is consistent with the numerical simulations. Note that another resonance occurs near 8.3 μm for each transmission spectrum which could be attributed to a parasitic large scale pattern due to the fabrication process that has been observed in SEM images of the samples.

Finally, we study numerically and experimentally the angular behavior of the filters. FEM simulations of the diffraction problem for incident angles between 0 and 30 degrees are reported as a transmission diagram in the space (β, ω) in Fig. 3 for TM (a) end TE (b) polarization. We also computed eigenfrequencies for different values of β and superposed the so-called dispersion diagram for the corresponding modes in Fig. 3. In both cases, the position of the transmission resonance peak is almost constant while its intensity slightly increases (resp. decreases) in TM (resp. TE) polarization. These main resonances can be attributed to the excitation of the previously studied waveguide mode because the position of the real part of the associated eigenvalue matches the position of the transmission maximum [see solid white curve on Fig. 3(a) for the TM mode and on Fig. 3(b) for the TE mode]. Note that unlike surface wave resonances, this resonance is a zeroth order Fabry–Perot resonance and hence has a position that is independent of the angle of incidence [10]. The spectral width of the transmission peak is also almost constant with β, which is confirmed by the study of the imaginary parts of the eigenfrequencies. In addition, a secondary resonant dip appears only in TM polarization and its position redshifts when β increases. This dip is due to the excitation of the delocalized surface plasmon mode whose dispersion diagram is reported in Fig. 3(a) (dashed white curve). The displacement of the dip with β matches the evolution of the real part of the eigenfrequency associated with this mode. This surface plasmon line is excited only in nonnormal incidence in TM polarization due to the symmetry of the mode at stake. Measurements are in good agreement with simulations [see Figs. 3(c) and 3(d)], even if the experimental main resonance is slightly blueshifted as previously noted. Moreover the transmission dip in the TM case is also present on the experimental data, although less apparent because the blueshift of the main resonance makes the overlap between this broad resonant peak and the narrow plasmonic dip stronger, which may in turn makes the plasmonic line less distinguishable in experimental data. Both numerical and experimental results demonstrate that this kind of AAA-based filters provide an angular tolerance of 30 degrees.

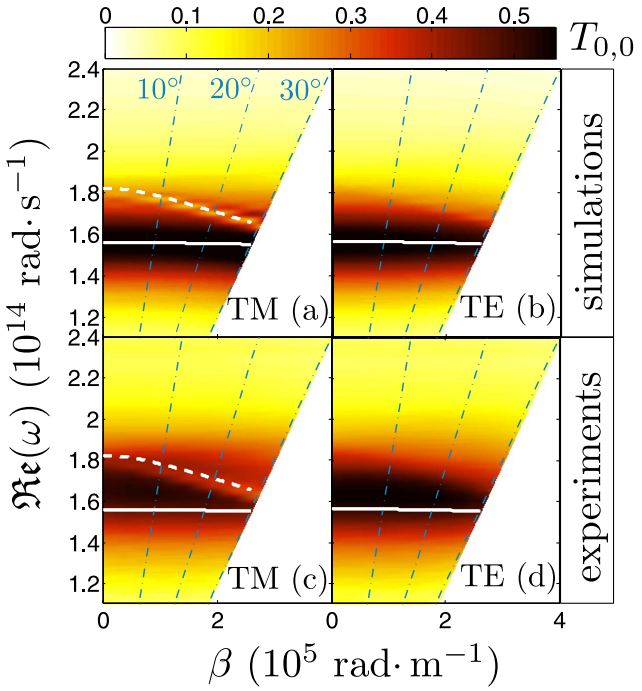

Fig. 3. Transmission diagrams for the filter M4. Colormap: transmission coefficient in the specular order $T_{0,0}$ as a function of frequency ω and transverse wavenumber β. Simulations: (a) TM and (b) TE polarization; measurements: (c) TM and (d) TE polarization. The thick solid and dashed lines represent the dispersion relation of the corresponding excited leaky modes. The thin dashed dotted lines indicates the incident angle θ_0 for the transmission diagram.

To conclude, we have studied both numerically and experimentally the resonant transmission properties of AAA-based transmission bandpass filters in the far infrared range for multispectral imaging applications. The transmission characteristics of the filter can be tuned by changing the value of the transverse geometric parameters of the structures so that the different filters can be fabricated on the same substrate in a single lithography step, leading to a low-cost process. A modal analysis is used to compute quickly the features of the resonance and allows us to infer this transmission peak from the excitation of a leaky mode. The measured spectra are in good agreement with FEM simulations and demonstrate the angular tolerance up to 30 degrees of the fabricated filters.

This research was supported by the fundings of PACA regional council and the FEDER program. The filters were fabricated in the Planete CT-PACA platform.

References

1. F. Garcia-Vidal, L. Martin-Moreno, T. Ebbesen, and L. Kuipers, Rev. Mod. Phys. **82**, 729 (2010).
2. A. Moreau, G. Granet, F. Baida, and D. Van Labeke, Opt. Express **11**, 1131 (2003).
3. F. Baida, D. Van Labeke, G. Granet, A. Moreau, and A. Belkhir, Appl. Phys. B **79**, 1 (2004).
4. J. Salvi, M. Roussey, F. I. Baida, M.-P. Bernal, A. Mussot, T. Sylvestre, H. Maillotte, D. Van Labeke, A. Perentes, I. Utke, C. Sandu, P. Hoffmann, and B. Dwir, Opt. Lett. **30**, 1611 (2005).
5. D. V. Labeke, D. Gérard, B. Guizal, F. I. Baida, and L. Li, Opt. Express **14**, 11945 (2006).
6. F. I. Baida, A. Belkhir, D. V. Labeke, and O. Lamrous, Phys. Rev. B **74**, 205419 (2006).
7. Y. Poujet, J. Salvi, and F. I. Baida, Opt. Lett. **32**, 2942 (2007).
8. W. Fan, S. Zhang, K. J. Malloy, and S. R. J. Brueck, Opt. Express **13**, 4406 (2005).
9. W. Fan, S. Zhang, B. Minhas, K. J. Malloy, and S. R. J. Brueck, Phys. Rev. Lett. **94**, 033902 (2005).
10. A. Roberts, Opt. Express **18**, 2528 (2010).
11. L. Lin and A. Roberts, Appl. Phys. **97**, 061109 (2010).
12. A. Di Falco, Y. Zhao, and A. Alú, Appl. Phys. **99**, 163110 (2011).
13. B. Vial, G. Demésy, F. Zolla, A. Nicolet, M. Commandré, C. Hecquet, T. Begou, S. Tisserand, S. Gautier, and V. Sauget, J. Opt. Soc. Am. B **31**, 1339 (2014).
14. P. Lalanne, J. P. Hugonin, and P. Chavel, J. Lightwave Technol. **24**, 2442 (2006).
15. V. Grigoriev, S. Varault, G. Boudarham, B. Stout, J. Wenger, and N. Bonod, Phys. Rev. A **88**, 063805 (2013).
16. A. L. Fehrembach and A. Sentenac, Appl. Phys. Lett. **86**, 121105 (2005).
17. Y. Ding and R. Magnusson, Opt. Express **12**, 1885 (2004).
18. G. Demésy, F. Zolla, A. Nicolet, and M. Commandré, Opt. Lett. **34**, 2216 (2009).
19. G. Demésy, F. Zolla, A. Nicolet, and M. Commandré, J. Opt. Soc. Am. A **27**, 878 (2010).
20. M. A. Ordal, R. J. Bell, J. R. W. Alexander, L. L. Long, and M. R. Querry, Appl. Opt. **24**, 4493 (1985).
21. E. D. Palik, *Handbook of Optical Constants of Solids* (Academic, 1991).
22. J.-P. Berenger, J. Comput. Phys. **114**, 185 (1994).
23. B. Vial, F. Zolla, A. Nicolet, M. Commandré, and S. Tisserand, Opt. Express **20**, 28094 (2012).
24. B. Vial, F. Zolla, A. Nicolet, and M. Commandré, Phys. Rev. A **89**, 023829 (2014).